Proceedings of the ASME 2017 Internal Combustion Engine Fall Technical Conference
ICEF2017
Oct 15-18, 2017, Seattle, Washington, USA

ICEF2017-3607

SPRAY-WALL INTERACTIONS IN A SMALL-BORE, MULTI-CYLINDER ENGINE OPERATING WITH REACTIVITY-CONTROLLED COMPRESSION IGNITION

Martin L Wissink
Oak Ridge National Laboratory
Oak Ridge, Tennessee, USA

Scott J Curran
Oak Ridge National Laboratory
Oak Ridge, Tennessee, USA

Chaitanya Kavuri
University of Wisconsin, Madison
Madison, Wisconsin, USA

Sage L Kokjohn
University of Wisconsin, Madison
Madison, Wisconsin, USA

ABSTRACT

Experimental work on reactivity-controlled compression ignition (RCCI) in a small-bore, multi-cylinder engine operating on premixed iso-octane and direct-injected n-heptane has shown an unexpected combustion phasing advance at early injection timings, which has not been observed in large-bore engines operating under RCCI at similar conditions. In this work, computational fluid dynamics (CFD) simulations were performed to investigate whether spray-wall interactions could be responsible for this result. Comparison of the spray penetration, fuel film mass, and in-cylinder visualization of the spray from the CFD results to the experimentally measured combustion phasing and emissions provided compelling evidence of strong fuel impingement at injection timings earlier than −90 crank angle degrees (°CA) after top dead center (aTDC), and transition from partial to full impingement between −65 and −90°CA aTDC. Based on this evidence, explanations for the combustion phasing advance at early injection timings are proposed along with potential verification experiments.

INTRODUCTION

Reactivity-controlled compression ignition (RCCI) is a dual-fuel combustion mode that uses in-cylinder fuel stratification to dictate the phasing and duration of a kinetically-controlled combustion event, which can result in low NO_x and soot and improved efficiency relative to conventional diesel combustion [1, 2]. RCCI relies on a significant difference in reactivity (autoignition propensity) between the two fuels, but the importance of various physical properties of the fuels in this combustion mode is currently unknown and is a subject of ongoing investigation [3]. RCCI most commonly uses a lean, premixed charge of low-reactivity fuel (e.g gasoline) via port injection or direct injection (DI) during the intake stroke along with DI of a higher reactivity fuel (e.g. diesel) relatively early in the compression stroke. Most research studies on RCCI have used diesel engine platforms, often with high pressure common rail diesel fuel injection systems [2]. These injectors typically feature wide spray angles which are well suited for mixing-controlled combustion mixture formation and are paired with highly-featured pistons to guide the fuel spray. The potential of spray interactions with the cylinder wall when using early DI for highly-premixed combustion strategies could have impacts on performance and durability, and therefore have the potential to limit the range of usable DI timings with certain fuel and hardware combinations.

While early DI timings are common in spark-ignited engines and many studies have investigated potential wall impingement and piston wetting as a source of hydrocarbons and particulate matter [4], there are relatively few examples of similar work with low-temperature combustion (LTC) compression ignition strategies. Previous studies into multi-cylinder RCCI have typically limited the earliest SOI timings to no earlier than about −70 crank angle degrees (°CA) after top

dead center (aTDC) [2]. Other LTC modes such as gasoline compression ignition (GCI) can also use early DI timings, as shown in Figure 1.

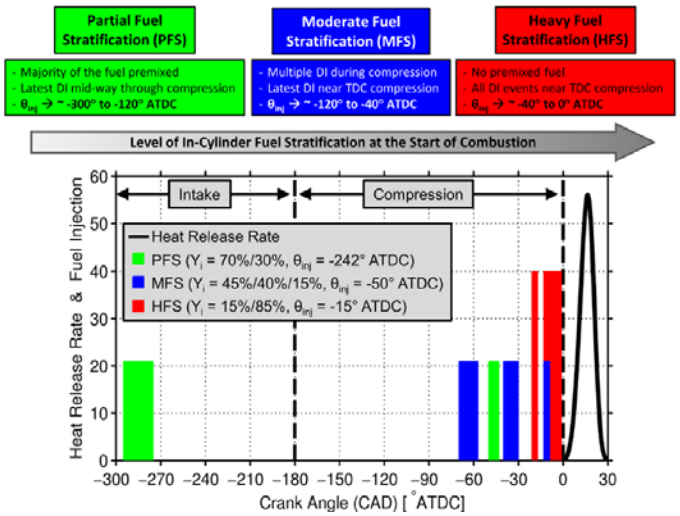

Figure 1. Descriptions and definitions of the three bins of fuel stratification for GCI and examples of common fuel injection strategies in relation to the intake stroke, compression stroke, and combustion heat release rate from Dempsey et al. [5]

A GCI study by Dempsey et al. [6], investigated the use of early DI timings ranging from about −90°CA aTDC to as early as −324°CA aTDC with volatile fuels to achieve highly premixed conditions, which were followed by a main injection closer to top dead center (TDC). The effects of spray-wall interactions were not the focus of that paper, but the authors did note that significant adjustments to the main injection were required to compensate for changes to combustion phasing as the first injection timing was moved beyond intake valve closing (IVC). The authors interpreted this result by noting, "The latest pilot injection timings (−126° and −91° ATDC) occur after the intake valve has closed, when the chamber is expected to be relatively quiescent and mixing rates are low… these fuel injection events are going to target the cylinder liner and most likely lead to fuel impingement on the liner, resulting in high HC emissions. On the contrary, the pilot injection timings that occur while the intake valve is open likely experience faster breakup, vaporization, and mixing with the incoming air. Even though these timings target the cylinder liner, they might not impinge on the liner and thus lead to more complete combustion." Purpose-built LTC engine concepts such as Delphi's GDCI engine [7] have undergone substantial optimization of the injection system and combustion chamber geometry to avoid or minimize both piston and wall wetting, but a significant part of that design involves limiting the SOI window.

A recent study by Wissink et al. employed wide sweeps of DI timing to explore the transition regions surrounding the RCCI regime under different levels and types of stratification [3], with a broader aim of isolating the effects of reactivity stratification from those of equivalence ratio and temperature stratification and improving our understanding of which fuel properties will be important for the further development of advanced combustion modes. That work utilized DI timings ranging from as early as −180°CA aTDC, which would be expected to result in a highly premixed charge, to as late as 10°CA aTDC, which resulted in partially mixing-controlled combustion. Previous RCCI studies exploring DI timings before −100°CA aTDC on a large-bore, heavy-duty engine have shown a tendency of the combustion phasing and emissions to asymptote to values near the equivalent homogeneous charge compression ignition (HCCI) condition [8]. However, in the range of DI timings expected to result in a highly premixed charge, unexpected non-asymptotic behavior in combustion phasing and emissions was observed in the small-bore engine used by Wissink et al. (the same engine and injectors as used by Dempsey et al. [6]), leading to questions about potential wall impingement. The present study investigates those potential spray-wall interactions by comparing the experimental results from the previous work with computational fluid dynamics (CFD) modeling using the same geometry and conditions.

METHODS

Experimental Setup

The experimental results reproduced here are a small subset of those shown in previous work by Wissink et al. [3], which presents the experimental setup and operating conditions in detail. A brief description relevant to the cases of interest in the present study will be provided here.

Table 1. Specifications of a 2007 GM 1.9 L multi-cylinder diesel engine

Number of cylinders	4
Bore [mm]	82.0
Stroke [mm]	90.4
Connecting rod length [mm]	145.4
Displacement [L]	1.91
Compression ratio [-]	16.5
IVO [°CA aTDC]	344
IVC [°CA aTDC]	−132
EVO [°CA aTDC]	116
EVC [°CA aTDC]	−340
Rated power [kW]	110
Rated torque [Nm]	315

Experiments were performed on a 2007 GM 1.9L 4-cylinder diesel engine using the stock diesel pistons. Engine specifications are provided in Table 1. Fuel injection system properties are provided in Table 2.

Table 2. DI fuel injector geometry

Number of holes (-)	7
Hole size (mm)	0.140
Included spray angle (°)	148

Figure 2 shows the engine layout, air handling topology, and fuel system layout. Direct injected fuel was delivered using the stock, common-rail (CR), solenoid-type, DI system. Premixed fuel was delivered using port fuel injection (PFI) into the intake manifold. All experiments were performed with combinations of gasoline primary reference fuels n-heptane (PRF0) and iso-octane (PRF100), with properties shown in Table 3.

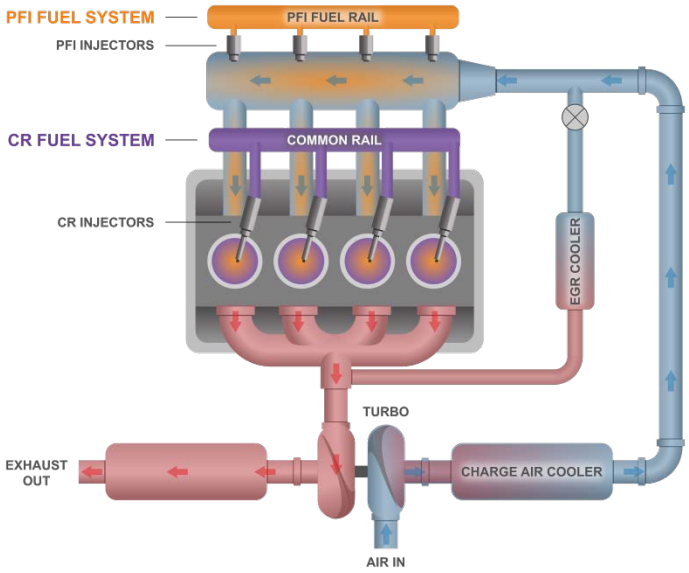

Figure 2. Diagram of the multi-cylinder GM 1.9 L engine

Table 3. Fuel properties

Property	**Fuel**	
	iso-octane (PRF100)	**n-heptane (PRF0)**
Formula	C_8H_{18}	C_7H_{16}
Research octane number	100	0
Motor octane number	100	0
Cetane number	11-19	53-54
Lower heating value [kJ/g]	44.3	44.6
Boiling point [°C]	99.2	98.38
Density [kg/m^3] (20°C)	691.9	683.7
Heat of vaporization [kJ/kg] (25°C/boiling point)	267/308	317/365

The experimental conditions for the experiments of interest are provided in Table 4. These consist of a sweep of DI start of injection (SOI) timing, referred to here as the RCCI experiment, and an HCCI baseline case. In the RCCI experiment, neat PRF0 was direct-injected into a premixed charge of PRF100. The fueling quantities were set such that 80% of the total fuel (by liquid volume) was PRF100, resulting in a global PRF of 80. For the HCCI experiment, PRF80 fuel was prepared externally by splash blending 20% PRF0 and 80% PRF100 (by liquid volume). The PRF80 fuel was delivered through the PFI system, and the engine was operated at 100% premix ratio (no DI), resulting in the same global PRF and equivalence ratio as the RCCI experiment. All cases were performed with the same boundary conditions, fixed fuel energy of 2100 J/cycle, and an engine speed of 2000 rev/min.

Table 4. Experimental conditions for DI SOI sweeps

Experiment	RCCI	HCCI
DI fuel	PRF0	-
PFI fuel	PRF100	PRF80
Premix ratio [%]	80	100
Premix ϕ [-]	0.28	0.35
Global PRF	80	80
DI SOI [°CA aTDC]	Start = −180 or stability limit End = PPRR limit (>15 bar/°CA) or combustion efficiency limit (<80%)	
DI fuel pressure [bar]	450	
Speed [RPM]	2000	
Global ϕ [-]	0.35 (No EGR)	
Fuel rate [J/cycle]	2100 (525/cylinder)	
BMEP [bar]	≈3.25	
T_{in} [°C]	40	
P_{in} [bar]	≈1.04	
Air rate [g/s]	≈35 (8.75/cylinder)	
EGR [%]	0	

Computational Modeling

Computational modeling was performed using an in-house CFD code based on the KIVA family of codes. The code includes improved physical and chemistry models developed at the University of Wisconsin's Engine Research Center [9]. The chemistry calculations were performed using a sparse analytical Jacobian solver coupled to the code, called SpeedChem [10, 11]. A reduced reaction mechanism made up of 80 species and 349 reactions is used to model the fuel chemistry [12]. This mechanism has been extensively validated and shown to accurately predict ignition delay and laminar flame speeds for gasoline PRF blends over a range of conditions.

The spray model uses the Lagrangian-Drop and Eulerian-Fluid (LDEF) approach. The Gasjet model of Abani et al. [13] [14] is used to model the relative velocity between the droplets and gas phase in the near nozzle region. The Kelvin Helmholtz-Rayleigh Taylor (KH-RT) model is used to model the spray break-up [15]. Turbulence is modeled using the Re-Normalization Group (RNG) k-ε model [16]. Munnanur's [17] droplet collision model is used. This model includes a comprehensive list of collision outcomes and considers effects of bounce, coalescence, fragmenting and non-fragmenting separations.

The wall film sub-model developed by O'Rourke and Amsden [18] was used to model droplet interaction with wall.

In this model, two regimes of spray wall interaction were considered: stick and splash. The transition between the regimes is identified based on the droplet Weber number estimated from the normal velocity of the droplet. The splash criterion accounted for the effects of film thickness. The splashing droplet mass, size and velocities were determined from empirical relations to match the experimental data from Yarin et al. [19] and Mundo et al. [20]. The direction of the splashing droplet velocity was estimated based on the results from Naber and Reitz [21].

The computational grid used for the current study is shown in Figure 3. The grid represents a 51.42° sector mesh, which includes one spray hole from the 7-hole injector described in Table 1. The grid is made up of ≈35,000 cells at bottom dead center (BDC) with a cell size of 1.25 mm in the axial and vertical directions and 2.5° in the azimuthal direction. Simulations were performed from IVC to exhaust valve opening (EVO). In the simulations, the PFI fuel was modeled as a completely homogenous mixture at IVC.

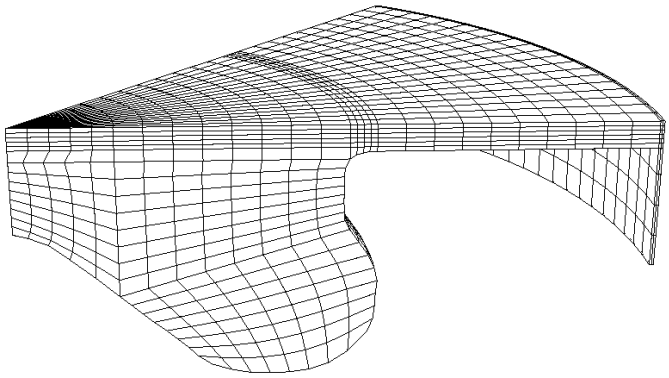

Figure 3. Computational grid used in the present study

The CFD model was thoroughly validated through comparisons with experiments before it was used in the study. Extensive spray model validation has been performed using the current CFD code and the code has been shown to adequately capture spray penetration and fuel distributions at conditions similar to the present study. Examples of spray model validation with the current code can be found in Chuahy and Kokjohn [22]. Examples of model validation under combusting conditions over a range of operating conditions can be found in Kavuri et al. [23, 24]. The agreement of the CFD results with the experimental data for the current study is shown in the following section.

RESULTS AND DISCUSSION

Combustion Phasing and Emissions Divergence

Figure 4 shows the measured and predicted combustion phasing, as measured by the crank angle at 50% of total heat release (CA50). The CA50 values shown for experimental cases are the average CA50 across all four cylinders. Both cyclic and cylinder-to-cylinder variability were discussed in previous work [3], but do not change the trends presented in this work and have been omitted from the figure for clarity.

Figure 4 shows that the measured CA50 from the RCCI SOI timing sweep does not asymptote to a CA50 value near the HCCI value as SOI was advanced. Note that, while the entire experimental DI SOI sweep is referred to as “Experiment RCCI” for the sake of brevity, only a subset of the SOI range could actually be considered RCCI. If we adopt a working definition of the actual RCCI region as that having a roughly linear negative slope, we observe that it extends from −65 to −35°CA aTDC. At −65°CA aTDC, the magnitude of the slope decreases, and a local maxima of CA50 is reached at −80°CA aTDC, which is advanced by more than 2 CAD relative to the HCCI value. While the primary focus of the CFD study was to capture the spray penetration rather than combustion behavior, it is worth noting that the CA50 trend is fully divergent between experiment and model at −90°CA aTDC. We can then adopt this point and the point at which the slope first changes in the experimental sweep (−65°CA aTDC) as nominal boundaries for the range in which we would first expect to see the source of this divergent behavior.

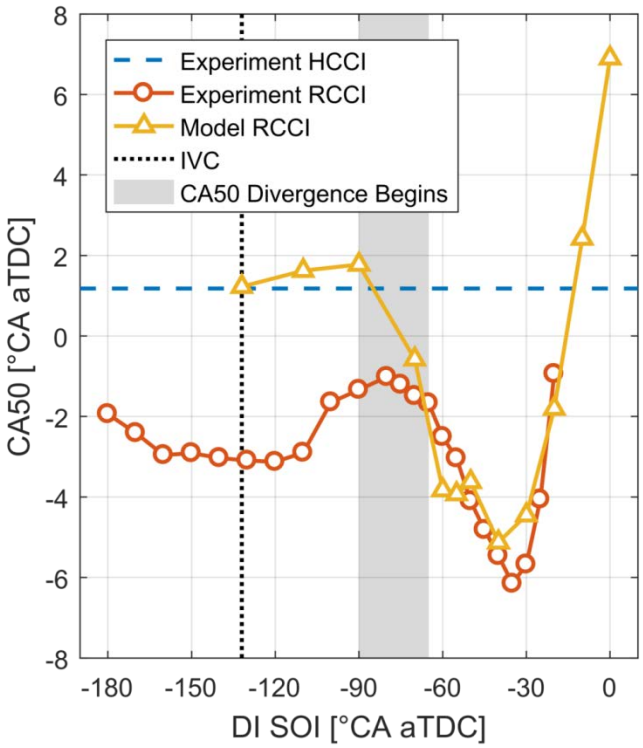

Figure 4. Combustion phasing of experimental HCCI and RCCI cases along with modeled RCCI. Nominal IVC location is indicated by vertical dashed line, and region in which divergence of experimental CA50 begins is indicated by shaded vertical bar.

For SOI timings more advanced than the range in which divergence is first observed, CA50 first advances, then levels off near IVC. Near BDC, CA50 begins to retard slightly. It is

plausible that turbulence associated with the valve closure event has some interaction with whatever phenomena is causing the CA50 advance at early SOI, but that possibility cannot be investigated with the closed-cycle model used in the present study. The previous study by Dempsey et al. also noted that injections that occur while the intake valve is open likely experience enhanced mixing effects [6].

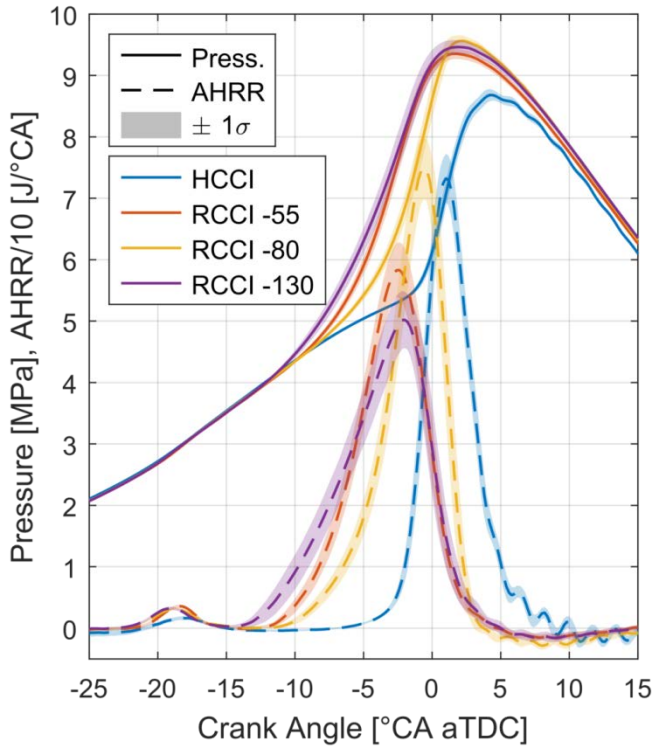

Figure 5. Ensemble-average pressure and heat release traces with standard deviation bands for selected experimental cases. Numbers next to RCCI cases in legend refer to DI SOI in units of °CA aTDC. All data are taken from cylinder 2.

To better understand the trends observed for CA50, the pressure and heat release traces for select experimental cases are shown in Figure 5. These include the HCCI case and three DI SOI timings from the RCCI sweep: −130°CA aTDC, which is the point closest to IVC, −80°CA aTDC, which is the local maxima for CA50, and −55°CA aTDC, which is in the actual RCCI regime and has the same CA50 as the case at IVC. As the DI SOI timing in the RCCI sweep is advanced from −55 to −80°CA aTDC, the CA50 and peak heat release rate move toward the HCCI trace, but there are still notable differences in the heat release characteristics. In particular, the magnitude of low-temperature heat release (LTHR) is higher than the HCCI case. Additionally, the slope at the start of high temperature heat release (HTHR) is more gradual for the RCCI cases, leading to longer overall combustion duration. Both of these observations indicate that there is still substantial reactivity stratification for the −80°CA aTDC case.

The subsequent observation that the −130°CA aTDC case still maintained elevated LTHR and had even longer combustion duration than the −55°CA aTDC case would then indicate that there is a greater degree of stratification at −130°CA aTDC despite the more advanced injection timing.

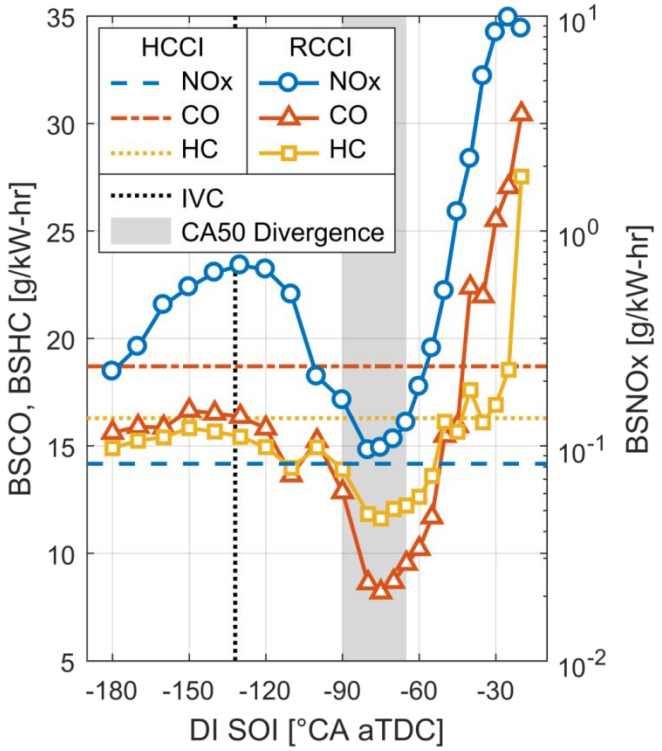

Figure 6. Emissions results of experimental HCCI and RCCI cases. BSCO and BSHC are shown on the left axis with linear scale, while $BSNO_x$ is shown on the right axis with logarithmic scale. Nominal IVC location is indicated by vertical dashed line, and region in which divergence of experimental CA50 begins is indicated by shaded vertical bar.

The increase in stratification for advanced SOI timings, although unintuitive, is supported by the experimental brake-specific emissions results, which are presented in Figure 6. In this figure, CO and HC are shown on the left axis in linear scale, and NO_x is shown on the right axis in logarithmic scale. When the SOI timing is later than −65°CA aTDC, we find that all three emissions increase with retarding DI SOI, consistent with increased stratification. The increase in NO_x with increased stratification can be explained by the dependence of adiabatic flame temperature on equivalence ratio (i.e., as stratification is increased, more regions exist in the high adiabatic flame temperature zone with $0.5 \leq \phi \leq 1.2$). Conversely, the increase in HC and CO can be explained by that fact that, as the stratification increases, less of the direct-injected n-heptane is mixed with the premixed iso-octane. Accordingly, increasing stratification decreases the reactivity of the premixed fuel (i.e., PRF100) due to both higher local PRF

number and lower local equivalence ratio. By the same logic, an increase in reactivity stratification could explain the increase in all three emissions that was observed as SOI was advanced from −80°CA aTDC to IVC. The decrease in emissions as SOI was advanced beyond IVC, along with the corresponding CA50 retard shown in Figure 4, therefore indicate that stratification is decreasing in this region. The region in which the trend reversal occurs for the emissions also coincides with the region in which CA50 divergence begins, which suggests a common cause for these effects.

CFD Spray Predictions

The CFD predictions are used to explain the experimentally observed trends. Figure 7 shows the peak spray penetration and the peak value of the direct injected mass in the fuel film predicted by the CFD model. The peak penetration is defined by locating the fuel droplet which causes the accumulated liquid mass to exceed 95% of the total liquid mass. The peak spray penetration increases linearly as DI SOI is advanced within the RCCI region, and begins to asymptote just as the region corresponding to CA50 divergence is entered. At the left edge of that same region, the peak spray penetration has been maximized (i.e., the liquid is impinging on the cylinder liner). With the exception of a small bump near −30°CA aTDC, the fuel film is essentially zero for all DI SOI after and including −60°CA aTDC. For more advanced injection timings, the DI fuel film mass increases rapidly. The region in which this change occurs overlaps with the region in which CA50 divergence begins.

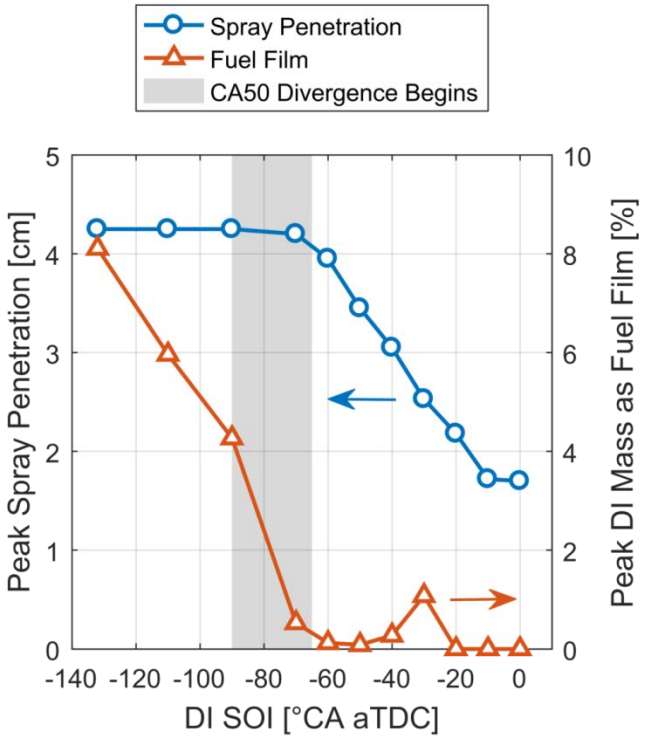

Figure 7. Peak spray penetration and peak mass of DI fuel film predicted by CFD. Region in which divergence of experimental CA50 begins is indicated by shaded vertical bar.

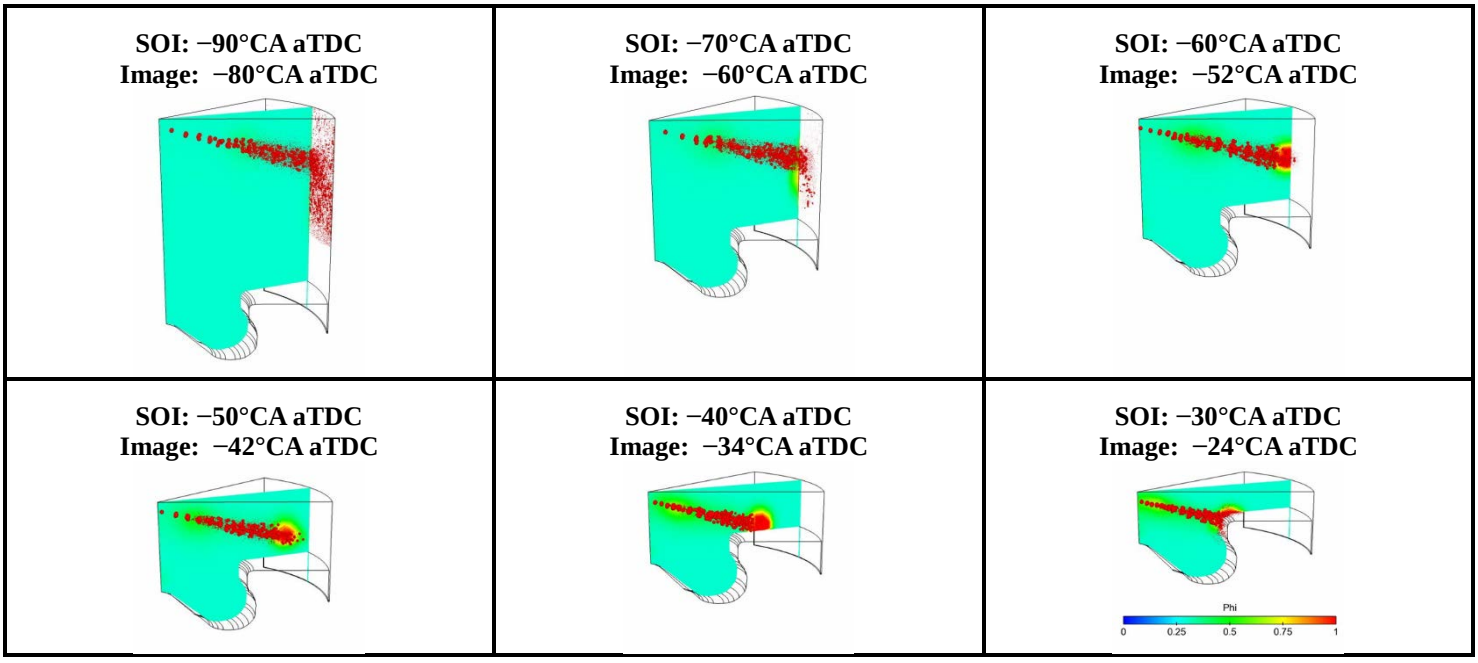

Figure 8. In-cylinder visualizations of spray parcels (red dots) and equivalence ratio (contour on cut-plane through spray axis) at SOI spanning the RCCI regime and the start of experimental CA50 divergence. Crank angle of each image is representative of the maximum spray penetration for each SOI.

Figure 8 shows a cut-plane coincident with the spray axis colored by equivalence ratio for the SOI timings spanning the RCCI regime and the start of experimental CA50 divergence. Starting with the SOI of −90°CA aTDC case in the top-left box, we observe that, at full spray penetration, a large amount of wall impingement is predicted. At an SOI timing of −70°CA aTDC, there is transitional behavior with a lower level of impingement, and at SOI of −60°CA aTDC, impingement is effectively negligible. For SOI between −60 and −30°CA aTDC, the spray is targeted to the squish region with minimal impingement, corresponding to the RCCI regime in the experiments. At an SOI timing of −30°CA aTDC, the spray directly targets and impinges on the lip of the piston, which was also seen in the fuel film results in Figure 7. For SOI retarded beyond −30°CA aTDC (not shown), the spray is contained within the bowl, and penetration continues to decrease due to increasing charge density and temperature, avoiding impingement. This qualitative interpretation of the spray visualization agrees with the trends seen in the peak spray penetration and peak fuel film mass shown in Figure 7.

Proposed Mechanism for Combustion Phasing Advance under Wall-Wetting Conditions

The experimental results indicate a divergence of both CA50 and emissions from a trajectory of continuously decreasing reactivity stratification with advancing DI SOI timing and strongly suggest that reactivity stratification is increasing as the DI SOI timing advances from −80 to −130°CA aTDC. The onset of wall wetting, indicated by the CFD results, coincides with the initial divergence of CA50 and emissions, and the decreasing charge density at earlier DI SOI agrees with the predicted trend that the peak mass of DI fuel in the wall film will continue to increase as DI SOI is advanced. This leads us to conclude that the most probable mechanism is as follows:

1. For sufficiently advanced DI SOI, fuel (n-heptane) is deposited on the wall. Further advance of DI SOI increases deposition on the wall.
2. Due to the relatively high volatility of n-heptane, nearly all of the fuel evaporates before ignition. Note that this is supported by the experiments as no significant change is seen in carbon balance as SOI timing is advanced (i.e., fuel does not appear to be entering the crank-case after impinging on the liner).
3. The deposition and evaporation process causes relatively high-reactivity regions to persist in the squish region at much later time than would otherwise occur in a non-wetting condition.

This model would therefore predict that once a wall-wetting condition is reached, further advance of DI SOI deposits more fuel, which leads to more high-reactivity fuel evaporating and being present in the squish region late in the compression stroke, which in effect creates a larger reactivity gradient. While there is no direct evidence at this time, it is also conceivable that the additional turbulence present with the intake valves open is responsible, either through reduction of impingement or faster evaporation, for the reversal of the CA50 and emissions trends for DI SOI before IVC.

Another consideration is that small amounts of high-reactivity oil could be participating in the ignition process. Two potential mechanisms for abstraction of oil from the wall film, illustrated in Figure 9, are drop ejection due to momentum exchange with the impinging fuel spray and evaporation of oil along with the deposited fuel. In either case, there are multiple ways of sampling the exhaust to determine if oil was introduced to the gaseous charge. In previous work using the same engine in this study, Storey et al. [25] reported measurements of long-chain alkanes by direct thermal desorption pyrolysis gas chromatography mass spectrometry (TDP-GC-MS) and measurements of lubricant metals by X-ray fluorescence (XRF). These techniques could be applied to compare operation of cases at matched CA50, such as DI SOI of −130 and −55°CA aTDC, in which we expect to have substantial wall-wetting in one case and none in the other. If a significantly higher amount of heavy alkanes or lubricant metals were detected at −130°CA aTDC, this would present direct evidence of oil participation, and strong indirect evidence of the fuel deposition model proposed here.

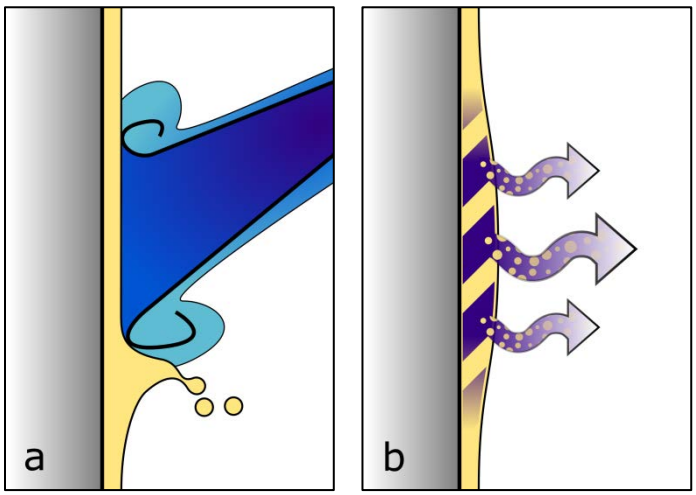

Figure 9. Possible mechanisms for abstraction of oil from the wall film: (a) Oil drop ejection due to momentum exchange, (b) Evaporation of oil along with deposited fuel

CONCLUSIONS

We have presented experimental evidence of a trend reversal of combustion phasing and brake-specific emissions of NO_x, HC, and CO for advanced direct injection timings of n-heptane, starting in the range of −65 to −90°CA aTDC. The results strongly suggest that from this starting range until IVC, advancing DI SOI results in increased reactivity stratification.

Spray penetration and fuel film calculations along with spray visualization from the CFD modeling indicate that wall wetting starts to occur within the same range as the CA50 and emissions transitions seen in the experimental results. The CFD modeling also predicts that the fuel film will continue to

increase as DI SOI is advanced beyond the point where wall wetting is first seen.

The experimental and modeling results lead us to propose a model in which n-heptane is deposited on the wall, and being relatively volatile, evaporates before ignition, resulting in a region of high reactivity in the squish region. Increased deposition on the wall would therefore lead to greater eventual reactivity stratification. We also proposed two mechanisms by which oil could be extracted from the wall film, therefore acting as a high-reactivity ignition source. A method of experimentally determining whether or not oil is participating in combustion was also proposed.

NOMENCLATURE

ϕ	Equivalence ratio
°CA	Crank angle degrees
AHRR	Apparent heat release rate
aTDC	After top dead center
BDC	Bottom dead center
BMEP	Brake mean effective pressure
BSCO	Brake-specific CO
BSHC	Brake-specific HC
$BSNO_x$	Brake-specific NO_x
CA50	Crank angle at 50% of total heat release
CO	Carbon monoxide
CFD	Computational fluid dynamics
CR	Common-rail
DI	Direct injection
DOE	Department of Energy
EGR	Exhaust gas recirculation
EVC	Exhaust valve closing
EVO	Exhaust valve opening
GCI	Gasoline compression ignition
HC	Hydrocarbons
HCCI	Homogeneous charge compression ignition
IVC	Intake valve closing
IVO	Intake valve opening
LTC	Low-temperature combustion
LTHR	Low-temperature heat release
NO_x	Oxides of nitrogen
PFI	Port fuel injection
PRF	Primary reference fuel
RCCI	Reactivity-controlled compression ignition
SOI	Start of injection
TDC	Top dead center
TDP-GC-MS	Thermal desorption pyrolysis gas chromatography mass spectrometry
XRF	X-ray fluorescence

ACKNOWLEDGMENTS

This research was conducted as part of the Co-Optimization of Fuels & Engines (Co-Optima) project sponsored by the U.S. Department of Energy (DOE) Office of Energy Efficiency and Renewable Energy (EERE), Bioenergy Technologies and Vehicle Technologies Offices. Co-Optima is a collaborative project of multiple national laboratories initiated to simultaneously accelerate the introduction of affordable, scalable, and sustainable biofuels and high-efficiency, low-emission vehicle engines.

This material is based on the work supported by the US Department of Energy, Office of Energy Efficiency and Renewable Energy, Vehicle Technologies Office via the Advanced Combustion Engine Systems program.

This research used resources at the National Transportation Research Center, a DOE Office of Energy Efficiency and Renewable Energy User Facility operated by the Oak Ridge National Laboratory.

REFERENCES

[1] Kokjohn, S., Hanson, R., Splitter, D., and Reitz, R., 2011, "Fuel reactivity controlled compression ignition (RCCI): a pathway to controlled high-efficiency clean combustion," International Journal of Engine Research, 12(3), pp. 209-226.

[2] Reitz, R. D., and Duraisamy, G., 2015, "Review of high efficiency and clean reactivity controlled compression ignition (RCCI) combustion in internal combustion engines," Progress in Energy and Combustion Science, 46, pp. 12-71.

[3] Wissink, M. L., Curran, S. J., Roberts, G., Musculus, M. P., and Mounaïm-Rousselle, C., 2017, "Isolating the effects of reactivity stratification in reactivity-controlled compression ignition with iso-octane and n-heptane on a light-duty multi-cylinder engine," International Journal of Engine Research, In Review.

[4] Stanglmaier, R. H., Li, J., and Matthews, R. D., 1999, "The Effect of In-Cylinder Wall Wetting Location on the HC Emissions from SI Engines," No. 1999-01-0502, SAE Technical Paper.

[5] Dempsey, A. B., Curran, S. J., and Wagner, R. M., 2016, "A perspective on the range of gasoline compression ignition combustion strategies for high engine efficiency and low NOx and soot emissions: Effects of in-cylinder fuel stratification," International Journal of Engine Research, 17(8), pp. 897-917.

[6] Dempsey, A. B., Curran, S., Wagner, R., and Cannella, W., 2015, "Effect of Premixed Fuel Preparation for Partially Premixed Combustion With a Low Octane Gasoline on a Light-Duty Multicylinder Compression Ignition Engine," Journal of Engineering for Gas Turbines and Power, 137(11), pp. 111506-111506-111512.

[7] Sellnau, M., Foster, M., Moore, W., Sinnamon, J., Hoyer, K., and Klemm, W., 2016, "Second Generation GDCI Multi-Cylinder Engine for High Fuel Efficiency and US Tier 3 Emissions," SAE International Journal of Engines, 9(2016-01-0760), pp. 1002-1020.

[8] DelVescovo, D., Kokjohn, S., and Reitz, R., 2017, "The Effects of Charge Preparation, Fuel Stratification, and Premixed Fuel Chemistry on Reactivity Controlled Compression Ignition (RCCI) Combustion," SAE International Journal of Engines, 10(2017-01-0773).

[9] Amsden, A. A., 1999, "KIVA-3V, release 2, improvements to KIVA-3V," Los Alamos National Laboratory, Los Alamos, NM, Report No. LA-UR-99-915.

[10] Perini, F., Galligani, E., and Reitz, R. D., 2012, "An Analytical Jacobian Approach to Sparse Reaction Kinetics for Computationally Efficient Combustion Modeling with Large Reaction Mechanisms," Energy & Fuels, 26(8), pp. 4804-4822.
[11] Lim, J. H., and Reitz, R. D., 2014, "High Load (21 Bar IMEP) Dual Fuel RCCI Combustion Using Dual Direct Injection," Journal of Engineering for Gas Turbines and Power, 136(10), pp. 101514-101514-101510.
[12] Wang, H., Deneys Reitz, R., Yao, M., Yang, B., Jiao, Q., and Qiu, L., 2013, "Development of an n-heptane-n-butanol-PAH mechanism and its application for combustion and soot prediction," Combustion and Flame, 160(3), pp. 504-519.
[13] Abani, N., Munnannur, A., and Reitz, R. D., 2008, "Reduction of numerical parameter dependencies in diesel spray models," Journal of Engineering for Gas Turbines and Power, 130(3), p. 032809.
[14] Abani, N., Kokjohn, S., Park, S., Bergin, M., Munnannur, A., Ning, W., Sun, Y., and Reitz, R. D., 2008, "An improved spray model for reducing numerical parameter dependencies in diesel engine CFD simulations," No. 0148-7191, SAE Technical Paper.
[15] Beale, J. C., and Reitz, R. D., 1999, "Modeling spray atomization with the Kelvin-Helmholtz/Rayleigh-Taylor hybrid model," Atomization and sprays, 9(6).
[16] Han, Z., and Reitz, R. D., 1995, "Turbulence modeling of internal combustion engines using RNG κ-ε models," Combustion science and technology, 106(4-6), pp. 267-295.
[17] Munnannur, A., 2007, "Droplet Collision Modeling in Multi-dimensional Engine Spray Computation," PhD Thesis, University of Wisconsin, Madison.
[18] O'Rourke, P. J., and Amsden, A., 2000, "A spray/wall interaction submodel for the KIVA-3 wall film model," No. 2000-01-0271, SAE Technical Paper.
[19] Yarin, A., and Weiss, D., 1995, "Impact of drops on solid surfaces: self-similar capillary waves, and splashing as a new type of kinematic discontinuity," Journal of Fluid Mechanics, 283, pp. 141-173.
[20] Mundo, C., Sommerfeld, M., and Tropea, C., 1995, "Droplet-wall collisions: experimental studies of the deformation and breakup process," International journal of multiphase flow, 21(2), pp. 151-173.
[21] Naber, J., and Reitz, R. D., 1988, "Modeling engine spray/wall impingement," No. 880107, SAE Technical Paper.
[22] Chuahy, F. D., and Kokjohn, S. L., 2017, "Effects of the Direct-Injected Fuel's Physical and Chemical Properties on Dual-Fuel Combustion," Fuel, Submitted.
[23] Kavuri, C., Paz, J., and Kokjohn, S. L., 2016, "A comparison of Reactivity Controlled Compression Ignition (RCCI) and Gasoline Compression Ignition (GCI) strategies at high load, low speed conditions," Energy Conversion and Management, 127, pp. 324-341.
[24] Kavuri, C., Kokjohn, S. L., Klos, D. T., and Hou, D., 2016, "Blending the benefits of reactivity controlled compression ignition and gasoline compression ignition combustion using an adaptive fuel injection system," International Journal of Engine Research, 17(8), pp. 811-824.
[25] Storey, J., Curran, S., Dempsey, A., Lewis, S., Walker, N. R., Reitz, R., and Wright, C., 2015, "The Contribution of Lubricant to the Formation of Particulate Matter with Reactivity Controlled Compression Ignition in Light-Duty Diesel Engines," Emission Control Science and Technology, 1(1), pp. 64-79.